IEEE Access
Multidisciplinary ⋮ Rapid Review ⋮ Open Access Journal

Received 13 March 2023, accepted 11 April 2023, date of publication 24 April 2023, date of current version 28 April 2023.

Digital Object Identifier 10.1109/ACCESS.2023.3269503

RESEARCH ARTICLE

Singularity Handling for Unbalanced Three-Phase Transformers in Newton-Raphson Power Flow Analyses Using Moore-Penrose Pseudo-Inverse

JIYEON JANG, DOHUN KIM, AND INSU KIM, (Member, IEEE)
Department of Electrical Engineering, Inha University, Incheon 22212, South Korea

Corresponding author: Insu Kim (insu@inha.ac.kr)

This work was supported by the Energy Cloud Research and Development Program through the National Research Foundation of Korea (NRF) funded by the Ministry of Science, Information and Communication Technology (ICT) under Grant 2019M3F2A1073.

ABSTRACT Power systems consist of generators, transformers, loads, and distributed power sources interconnected through lines. The reliable operation of the system requires that voltage and current magnitudes, angles, and power flow are within allowable ranges. Several methodologies have been proposed to solve the power flow consisting of nonlinear algebraic equations. Among them, the Newton-Raphson method is widely used due to its simplicity in building the bus admittance matrix, high accuracy, and fast convergence. However, the method has several limitations, such as singularity issues that occur when some or all Jacobian matrix elements become zero. This prevents the power flow calculation from converging since the inversion of the Jacobian matrix cannot be obtained. To address this limitation, this study proposes a novel and robust power flow calculation methodology that can solve singularities for various ill conditions using the Moore-Penrose Pseudo-inverse. This method improves the classical Newton-Raphson method by addressing its shortcomings. The performance of the proposed algorithm was evaluated using various testbeds, including balanced and unbalanced radial systems, a large-scale power grid, and systems with ungrounded transformers. The accuracy of the proposed algorithm was verified by comparing the power flow calculation with DIgSILENT Power Factory. The testbed consisted of modified IEEE 4-, 13-, 37-, and 69-bus systems.

INDEX TERMS Moore-Penrose Pseudo-inverse, Newton-Raphson method, power flow analysis, singularity, three-phase transformer.

I. INTRODUCTION

The power system consists of numerous generators, transformers (TRs), loads, and distributed power sources interconnected through transmission lines. Several conditions must be met to ensure the reliable and secure operation of such a complex power system. These include maintaining bus voltages close to the rated voltage (e.g., ± 5 percent), matching power demand and supply, avoiding overloading of transmission lines and TRs, and ensuring that generators operate within their maximum power transmission limit. Power flow analysis, power flow calculation, is a technique used to verify whether the four conditions are satisfied. Power flow analysis can determine the voltage magnitude, phase angle, transmission power, and transmission loss of the power system operating in steady-state and take countermeasures to ensure stable power system operation.

The associate editor coordinating the review of this manuscript and approving it for publication was Elizete Maria Lourenco.

A. PREVIOUS STUDIES

Various methodologies are used to calculate power flow for power systems expressed in nonlinear algebraic equations, including Gauss-Seidel (GS), Newton-Raphson (NR), and Fast Decoupled Power Flow (FDPF). While the GS power-flow method was often used, it could have poor convergence and require extensive iteration processes. In response, the NR method was proposed to improve the convergence characteristics of the GS method [1]. The

power-flow calculations with the NR method can converge within a low number of iterations, often mitigating or avoiding these shortcomings (e.g., the convergence property) [1], [2]. Additionally, the NR method is relatively easier to build the bus admittance matrix (i.e., Ybus), ensuring high accuracy and fast convergence [1], [3]. As a result, the NR method has become more widely used for power-flow analyses [4].

Additionally, there are limitations to the NR method. The convergence speed for power flow calculations using the NR method depends on the initial settings, such as initial voltage magnitude and angle. The convergence rate is higher when the initial value is closer to the solution [5]. This implies that the power flow calculation using the NR method may fail depending on the initial setting value. Milano et al. [6] described an ill-conditioned system as a case where a solution exists, but the power flow calculation does not converge to a solution when the starting point is a flat initial condition (i.e., the magnitude of the voltage is 1 per unit [p.u.] and the phase angle of the voltage is 0 degrees). In such cases, the process of calculating the inversion of the Jacobian matrix in the NR method often approaches singularities [6], [7]. Consequently, the NR method-based calculation may not converge for ill-conditioned systems, leading to divergence [8].

The NR method has limitations where the power flow calculation may not converge due to various factors, not just the initial value. For instance, in large-scale power grids or distribution systems with high resistance to reactance (R/X) ratios, power flow calculations using the NR method often cannot converge [9]. Additionally, the NR method-based calculation can be problematic for analyzing unbalanced radial distribution systems because the power flow sometimes does not converge [3], [10]. Moreover, the NR method-based calculation is weak in ungrounded systems, which can be classified as ill-conditioned [11]. However, in actual power systems, ill-conditioned grids are prevalent, including large-scale grids, distribution systems with high R/X ratios, unbalanced grids, or ungrounded grids [12]. Therefore, calculating the power flow in such ill-conditioned grids is essential. Thus, improving and analyzing the performance of the power flow calculation method when the calculation using the NR method does not converge in an ill-conditioned system is necessary.

Numerous studies have been conducted to improve the performance of power flow calculation methods and to solve the convergence issues and singularities that may occur during the calculation process. For instance, Alves et al. proposed an improved FDPF method that injects reactive power into the selected P-V bus to handle singularities at the maximum loading point and solve non-convergence issues [13]. Although the FDPF method is similar to the NR method, since the NR method does not simplify the off-diagonal components of the Jacobian matrix, this improvement methodology cannot be judged applicable to the NR method, and the study is limited to solving the singularity at the maximum loading point [13]. Pourbagher et al. introduced the adaptive multi-step Levenberg-Marquardt (AMSLM) method to solve singularity issues in ill-conditioned systems, and Tostado et al. presented a modified NR method called NR-predictor-corrector (NR-PC) to improve convergence in well-conditioned and ill-conditioned systems [14], [15]. However, it is difficult to judge whether these studies improved the performance of the NR method [14], [15]. And in another study, through the successive approximation method (SAM) and the adomian decomposition method (ADM) applying the principles of equation formulation, abbreviated mapping, and fixed-point theorem, Dewangan et al. solved the singularities of the NR method-based calculation to improve the performance of power flow calculations [16]. In addition, a method has been proposed to inject various forms of perturbations to solve singularities caused by ill conditions of Jacobian matrices [17]. However, most of these studies only addressed singularities in unbalanced, radial, or distribution systems and did not necessarily improve the performance of the classical NR method-based calculations. Thus, Yi Zhang et al. improved the performance of power flow calculation in ungrounded distribution systems by solving the convergence problem of the NR methods in ungrounded networks by limiting the magnitude of the zero-sequence current to zero in an ungrounded bus [11]. In other words, this study dealt with the ill-condition problem of unground TRs and improved the NR method calculation performance. However, the study is insufficient to solve the problem of the ungrounded circuit of the NR method calculation in that only the inside of the distribution network is an ungrounded connection, and the ends are all ground connections [11]. In other words, previous studies are limited by the fact that they do not address issues such as ungrounded, unbalanced, overloaded, and radial in a unified way.

Although many studies have attempted to improve power flow calculation methods and address singularity issues, there remains a need for a more robust NR method that can handle various ill conditions, such as unbalanced radial distribution systems with ungrounded TR connections. While some studies have proposed modifications to the NR method, it is unclear if these methodologies can improve the performance of the NR method itself. To address this issue, this study introduces a novel approach that utilizes the singular value decomposition (SVD) method to solve the singularity problem during the inversion of the Jacobian matrix. By applying the Moore-Penrose Pseudo-inverse (MP-PI) with SVD [18], this study has developed a more robust NR method that improves power flow calculation performance in various ill-conditioned systems, including large-scale power grids and distribution systems with ungrounded TRs.

Previous studies have used MP-PI to find the solution to nonlinear algebraic power flow equations. However, some studies have not verified the accuracy of MP-PI-based calculations, and some studies have verified the accuracy of MP-PI-based calculations, but as pointed out in this study,

they have not dealt with MP-PI-based method for systems with various ill conditions in an integrated manner [3], [19], [20], [21].

This study highlights the significance of this novel approach by demonstrating its effectiveness in improving the performance of the NR method in various scenarios. In other words, this study addresses the performance improvement of the NR method itself and its integrated simulation and validation under various ill-condition. In Section III, this study provides a brief overview of the MP-PI method, while Section V presents an example of calculating the MP-PI in practice. Overall, this study makes a valuable contribution to the field by addressing a critical need for a more robust and reliable NR method that can handle various ill conditions in power system analysis.

B. CONTRIBUTIONS AND FINDINGS

Previous studies have proposed various approaches for solving singularities and finding valid solutions for nonlinear algebraic equations. Although many studies have successfully solved singularities in large-scale or radial distribution systems, ungrounded conditions are also one of the causes of singularities during NR-based power flow calculations. For instance, in an unbalanced system with unbalanced loads, the zero-sequence current (i.e., the unbalanced current) flows, and singularities often occur when the zero-sequence current cannot be defined in an ungrounded bus (e.g., a delta [D] connection) [22]. In other words, the singularities are sometimes caused by an ungrounded connection of the TR (i.e., the ungrounded wye [Y] or D-connections). Some studies have focused on solving the intuitive problem of singularity rather than improving the NR method, solving the singularity caused by ungrounded connection by methods such as grounding, capacitor banks, or shunt capacitance [23], [24], [25]. While these methodologies can often solve singularities, they may not necessarily improve the performance of the classical NR method. Therefore, novel alternatives are needed to improve the performance of the NR method while simultaneously solving singularities. Additionally, a robust methodology that can calculate power flow in a system containing various ill conditions, rather than each ill-condition separately, is required to address the challenge of singularities while improving the NR method.

Therefore, this study adopts MP-PI matrices to deal with singularities and develops an MP-PI-based singularity-solving NR-based algorithm in the MATLAB program. The proposed singularity-solving method can be applied when calculating the impedance matrix (Z_{bus}) for short-circuit analysis. The system impedance between the synchronous voltage and the fault point must be known to calculate the fault current caused by a short circuit or a fault. However, inverting the admittance matrix to find the impedance matrix is often impossible for singular admittance matrices through the classical NR method. But, the proposed MP-PI-based NR method can provide the bus impedance matrix even when the bus admittance matrix is non-invertible, e.g., a tap-changing TR. Furthermore, the MP-PI methodology is easy to apply and can improve the performance of many algorithms based on the NR method, thus providing convenience for NR method-based research.

II. PROBLEM STATEMENT

The Jacobian matrix is often singular and cannot be inverted when calculating the power flow using the classical NR method. Many studies have shown that singularities occur when solving nonlinear power flow equations of ill-condition power systems (e.g., the unbalanced radial distribution system). However, previous studies focused only on solving singularities and verified only specific ill-condition systems (e.g., the unbalanced or radial systems or maximum loading point). Or previous studies did not apply the proposed methodologies to the NR method [14], [26], [27], [28]. Thus, this study expanded the range for the ill-conditioned cases, which was often previously defined as a high R/X ratio or heavily loaded networks, adding ill-conditioned cases from the viewpoint of TRs to the validation case studies. The proposed MP-PI method was applied to the classical NR method to facilitate solving the singularities. This study set five testbeds (i.e., IEEE 4-, 13-, 37-, and modified 37-, modified 69-bus feeders) to solve the singularity of the power system with newly defined ill-conditioned cases based on TRs and to improve the convergence of the classical NR method. This study slightly modified the original IEEE test feeders to ensure that the proposed MP-PI-based singularity-solving methodology is applicable under various conditions. And this study used the DIgSILENT Power Factory software to confirm the accuracy of the MP-PI-based NR algorithm. The accuracy of the proposed MP-PI-based algorithm was verified by comparing the results of power flow calculation through DIgSILENT Power Factory, a verified power flow calculation software, and the developed MP-PI-based NR algorithm.

The remainder of this paper is organized as follows. Section III presents the proposed solution method. Section IV finds the singularity occurrence in ungrounded TRs, and Section V provides validation case studies. Section VI discusses the results and Section VII summarizes the paper.

III. PROPOSED METHOD

A. NEWTON-RAPHSON METHOD

The equation (1) represents a nonlinear algebraic equation as a matrix and such that solving the nonlinear algebraic equation is finding the value of $\boldsymbol{x}$ when $\boldsymbol{y}$ and $\boldsymbol{f(x)}$ are

$$f(x) = [f_1(x)\, f_2(x)\, f_3(x)\ \cdots f_n(x)]^T = y \tag{1}$$

and

$$y - f(x) = 0. \tag{2}$$

Adding $\boldsymbol{J} \cdot \boldsymbol{x}$ to both the left and right sides of the equation (2) and multiplying by $\boldsymbol{J^{-1}}$,

$$x = x + J^{-1}[y - f(x)], \tag{3}$$

and calculating $\boldsymbol{x(i+1)}$ on the left using the right $\boldsymbol{x(i)}$ from (3),

$$x(i+1) = x(i) + J^{-1}(i)[y - f(x(i))], \tag{4}$$

where $\boldsymbol{J(i)}$ is the Jacobian, an $n \times n$ matrix, with each element being a partial differential,

$$J(i) = \left.\frac{df}{dx}\right|_{x=x(i)} = \begin{bmatrix} \frac{\partial f_1}{\partial x_1} & \frac{\partial f_1}{\partial x_2} & \cdots & \frac{\partial f_1}{\partial x_n} \\ \frac{\partial f_2}{\partial x_1} & \frac{\partial f_2}{\partial x_2} & \cdots & \frac{\partial f_2}{\partial x_n} \\ \cdot & \cdot & & \cdot \\ \cdot & \cdot & & \cdot \\ \cdot & \cdot & & \cdot \\ \frac{\partial f_n}{\partial x_1} & \frac{\partial f_n}{\partial x_2} & \cdots & \frac{\partial f_n}{\partial x_n} \end{bmatrix}_{x=x(i)}. \tag{5}$$

The principle of the NR method is as follows. Let $\boldsymbol{x}$ be the value to find, then, the phase angle and voltage magnitude constitute the matrix of $\boldsymbol{x}$, and $\boldsymbol{x}$, $\boldsymbol{y}$, and $\boldsymbol{f(x)}$ matrices can be defined as, respectively,

$$x = [\delta V]^T = [\delta_2 \delta_3 \cdots \delta_n V_2 V_3 \cdots V_n]^T, \tag{6}$$

$$y = [PQ]^T = [P_2 P_3 \cdots P_n Q_2 Q_3 \cdots Q_n]^T, \tag{7}$$

and

$$\begin{aligned} f(x) &= [P(x)Q(x)]^T \\ &= [P_2(x)P_3(x)\cdots P_n(x)Q_2(x)Q_3(x)\cdots Q_n(x)]^T, \end{aligned} \tag{8}$$

where the active and reactive power expressions for $\boldsymbol{y}$ can be expressed as

$$\begin{aligned} y_k &= P_k = P_k(x) = V_k \sum_{m=1}^{n} Y_{km} V_m \cos(\delta_k - \delta_m - \theta_{km}) \\ y_{k+n} &= Q_k = Q_k(x) = V_k \sum_{m=1}^{n} Y_{km} V_m \sin(\delta_k - \delta_m - \theta_{km}) \\ k &= 2, 3, \ldots.., n (k = 1 means\ slack). \end{aligned} \tag{9}$$

Thus, the Jacobian matrix can be expressed as

$$J = \begin{bmatrix} J1 & J2 \\ J3 & J4 \end{bmatrix} = \begin{bmatrix} \frac{\partial P_2}{\partial \delta_2} & \cdots & \frac{\partial P_2}{\partial \delta_n} & \frac{\partial P_2}{\partial V_2} & \cdots & \frac{\partial P_2}{\partial V_n} \\ \vdots & \ddots & \vdots & \vdots & \ddots & \vdots \\ \frac{\partial P_n}{\partial \delta_2} & \cdots & \frac{\partial P_n}{\partial \delta_n} & \frac{\partial P_n}{\partial V_2} & \cdots & \frac{\partial P_n}{\partial V_n} \\ \frac{\partial Q_2}{\partial \delta_2} & \cdots & \frac{\partial Q_2}{\partial \delta_n} & \frac{\partial Q_2}{\partial V_2} & \cdots & \frac{\partial Q_2}{\partial V_n} \\ \vdots & \ddots & \vdots & \vdots & \ddots & \vdots \\ \frac{\partial Q_n}{\partial \delta_2} & \cdots & \frac{\partial Q_n}{\partial \delta_n} & \frac{\partial Q_n}{\partial V_2} & \cdots & \frac{\partial Q_n}{\partial V_n} \end{bmatrix} \tag{10}$$

and hence $\boldsymbol{x}$ converges and can be found iteratively through

$$\Delta y(i) = \begin{bmatrix} \Delta P(i) \\ \Delta Q(i) \end{bmatrix} = \begin{bmatrix} P - P(x(i)) \\ Q - Q(x(i)) \end{bmatrix}, \tag{11}$$

$$\begin{bmatrix} \Delta\delta(i) \\ \Delta V(i) \end{bmatrix} = \begin{bmatrix} J1(i) & J2(i) \\ J3(i) & J4(i) \end{bmatrix}^{-1} \begin{bmatrix} \Delta P(i) \\ \Delta Q(i) \end{bmatrix}, \tag{12}$$

and

$$x(i+1) = \begin{bmatrix} \Delta\delta(i+1) \\ \Delta V(i+1) \end{bmatrix} = \begin{bmatrix} \delta(i) \\ V(i) \end{bmatrix} + \begin{bmatrix} \Delta\delta(i) \\ \Delta V(i) \end{bmatrix}. \tag{13}$$

B. MOORE-PENROSE PSEUDO-INVERSE PRINCIPLE

An inverse matrix creates the identity matrix when multiplied by the original matrix, i.e.,

$$A^{-1}A = AA^{-1} = I(I : identity\ matrix). \tag{14}$$

For example, the general 2×2 matrices

$$A = \begin{bmatrix} a_1 & a_2 \\ a_3 & a_4 \end{bmatrix} \tag{15}$$

can be inverted as

$$A^{-1} = \frac{1}{\det(A)} \begin{bmatrix} a_4 & -a_2 \\ -a_3 & a_1 \end{bmatrix} = \frac{1}{a_1 a_4 - a_2 a_3} \begin{bmatrix} a_4 & -a_2 \\ -a_3 & a_1 \end{bmatrix}. \tag{16}$$

When the determinant for matrix $\boldsymbol{A}$ (i.e., $\det(\boldsymbol{A})$) in the equation (16) becomes zero, matrix $\boldsymbol{A}$ becomes singular. Any square matrix with at least one row or column of zeros is a singular matrix, and the inverse cannot be obtained. The MP-PI matrix uses the SVD method [29], providing something similar to the formal inverse matrix when the original inversion does not exist, and the MP-PI matrix can be used when there is no unique solution or many solutions.

The SVD method decomposes a matrix into singular vectors and values, e.g.,

$$A = UDV^T \tag{17}$$

where $\boldsymbol{A}$, $\boldsymbol{U}$, $\boldsymbol{D}$, and $\boldsymbol{V}$ are $n\times m$, $n\times n$, $n\times m$, and $m\times m$ matrices, respectively; the diagonal for $\boldsymbol{D}$ is an eigenvalue of $\boldsymbol{A}$; column vectors for $\boldsymbol{U}$ represent left-singular vectors; column vectors for $\boldsymbol{V}$ represent right-singular vectors; eigenvectors for $\boldsymbol{AA^T}$ are left-singular vectors, and eigenvectors for $\boldsymbol{A^TA}$ are right-singular vectors [30].

The MP-PI matrix $\boldsymbol{A^+}$ can be defined as

$$A^+ = VD^+U^T. \tag{18}$$

where $\boldsymbol{V}$ and $\boldsymbol{U}$ can be obtained through SVD and $\boldsymbol{D^+}$ by transposing non-zero components of the diagonal matrix $\boldsymbol{D}$ after taking the inverse. Thus, the following identities hold [31]

$$\begin{aligned} 1.&(A^+)^+ = A \\ 2.&(A^+)^T = (A^T)^+ \\ 3.&A^+AA^+ = A^+ \\ 4.&AA^+A = A. \end{aligned} \tag{19}$$

C. PROPOSED POWER FLOW ALGORITHM

The use of MATLAB software to find the MP-PI matrix can be disadvantageous due to the complicated calculation process. Although simple systems with a small number of nodes can be calculated quickly, for systems with many nodes (i.e., large-scale power systems), the calculation time can be significantly longer than the conventional inversion process. Therefore, the proposed MP-PI-based NR algorithm improves its performance (e.g., calculation speed) by minimizing calculation steps and time using the MP-PI matrix.

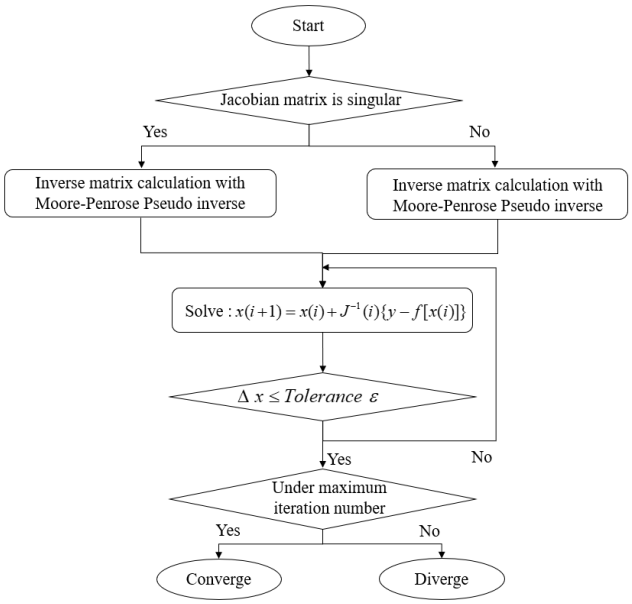

FIGURE 1. Proposed moore-penrose pseudo-inverse calculation-based Newton-Raphson algorithm flowchart.

The modified MP-PI-based NR algorithm finds the original inverse matrix when the Jacobian matrix is invertible and only uses the MP-PI matrix when the Jacobian matrix is noninvertible (i.e., singular) or nearly singular. Since the inversion calculation is also sensitive even when the Jacobian matrix is close to the singular matrix, this study calculated the inverse matrix through the MP-PI even when the Jacobian matrix is near singular. Fig. 1 shows the flowchart of the MP-PI-based NR algorithm proposed in this study, which improves the efficiency of the power flow calculation while ensuring accuracy. The convergence and computational speed of the proposed MP-PI-based calculation are shown in the Discussion section compared to the classical NR method.

The modified MP-PI-based NR algorithm has three advantages:

1) The MP-PI-based NR algorithm provides a viable solution even when the Jacobian matrix is noninvertible (i.e., singular), ensuring that power flow calculations converge.
2) The impedance matrix can be obtained by inverting the non-invertible admittance matrix, which can be useful for short-circuit analysis.
3) The conventional method of inverting the Jacobian matrix is employed when the matrix is invertible, improving overall calculation efficiency (e.g., calculation speed).

In other words, this study appropriately utilizes both the classical inversion and the MP-PI matrix.

IV. SINGULARITY IN THREE-PHASE TRANSFORMERS

A. UNGROUNDING

Conventional NR-based power flow calculations may not converge due to singularities, and many previous studies have shown that singularities occur during power flow calculation

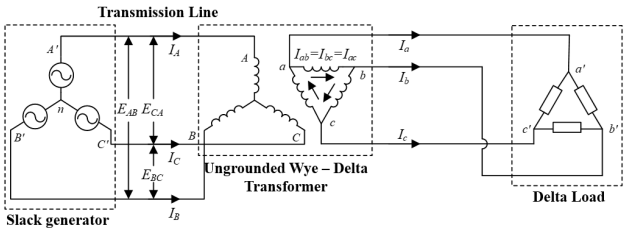

FIGURE 2. Simple three-phase power system diagram with an ungrounded wye-delta transformer.

for ill-conditioned systems and then subsequently try to solve the ill-condition problems. However, previous studies did not apply their proposed singularity-solving methodology to the NR method, the most used power flow calculation method, and verified only for a specific ill-condition system. In other words, when the proposed algorithms are confirmed for large power grids or distribution systems with high R/X ratios (i.e., commonly referred to as ill-condition), their algorithms are not verified for singularity problems from ill-condition systems with ungrounded three-phase TRs. In contrast, this study solved the singularity for ill-condition systems with ungrounded three-phase TRs.

Since the ungrounded connection of the TR has no ground references, the phase-to-ground voltage cannot be defined. Fig. 2 shows an example three-phase system including a Y-D ungrounded TR. Although arbitrarily defining a ground reference can often solve the singularity problem (i.e., no ground reference), this is sometimes theoretically inappropriate. Power-flow analysis can converge to a unique solution if the ground reference exists. However, when the ground reference is not defined, the solution for the power-flow analysis is not unique, often resulting in a singularity. Power flow calculation for ungrounded systems with ungrounded TRs (e.g., Y-D) or ungrounded connections (e.g., Y- or D-connections) also requires the ground reference to be defined. However, real world power networks often used ungrounded TRs, grid-connected inverters without a neutral connection, or ungrounded connections. Therefore, power flow calculations in systems with ungrounded TRs or ungrounded connections are essential.

B. ZERO-SEQUENCE NETWORK

The power flow calculation in a power system is typically based on the admittance matrix of the system. The admittance matrix is a square matrix that represents the network admittances and is used to calculate the nodal voltages and power flow. In terms of the TR connection, power systems can be divided into grounded and ungrounded systems.

In a grounded power system, the zero-sequence current can flow to the ground, and the magnitude of the current can be calculated using Kirchhoff's laws. The admittance matrix can then be calculated using positive and negative sequence components of the system admittances, and since the admittance matrix is invertible, a unique solution for the power flow can

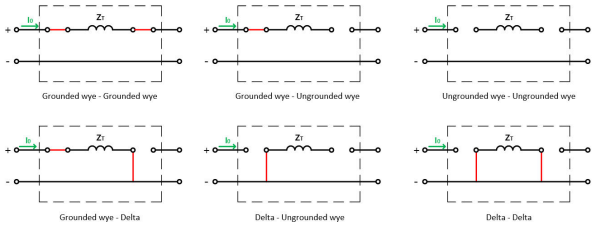

FIGURE 3. Zero-sequence networks of the 5-limb two-winding transformer according to the connection of both sides.

be obtained. However, in an ungrounded power system, the zero-sequence current cannot flow to the ground, and the flow is not well-defined. This results in a singularity in the calculation of the admittance matrix, meaning that the matrix cannot be inverted, and obtaining a unique solution for power flow calculations using conventional methods becomes difficult.

In conclusion, the singularity in power flow calculations that often occurs when a TR has an ungrounded connection is due to the impact of the zero-sequence current on the system admittance matrix. The inability to properly define the behavior of the zero-sequence current leads to a singularity in the admittance matrix calculation, making it challenging to obtain a unique solution for the power flow using a classical NR method.

Fig. 3 expresses the zero-sequence network of six types of 5-limb two-winding TRs according to the connection. In Fig. 3, Z_T means the TR impedance. First, in the case of a grounded wye-grounded wye (Yg-Yg) TR, the primary and the secondary sides are connected, and the TR impedance Z_T is between the two connections. However, in the case of a Yg-Y or Yg-D TR, the ungrounded secondary side is opened, and the primary and secondary sides are disconnected. Unlike the Yg-connection, the Y- or D-connection (i.e., an ungrounded connection) sides are opened in the zero-sequence network. The case of the D-connection differs from the ungrounded Y-connection in that the D-side is grounded to the reference. But the D-connection has in common with the Y-connection that the zero-sequence network becomes an open circuit. Therefore, the zero-sequence current cannot flow in the ungrounded systems, and singularities can occur for this reason. In other words, the linear summation of the line currents (e.g., $I_a + I_b + I_c$) in ungrounded systems (e.g., Y and D connections) is zero. When the unbalanced currents (e.g., $I_a + I_b + I_c \neq 0$) try to flow in an ungrounded network, however, the nonzero zero-sequence current (e.g., $I_0 = (I_a + I_b + I_c)/3 \neq 0$) cannot flow because of the opened zero-sequence network in ungrounded networks, which results in a singularity in calculating the power flow. Therefore, singularities can occur more often when calculating the power flow in an unbalanced system than in a balanced network.

As a result, this study confirmed the relationship between the three-phase TRs and the singularity of the inversion of the Jacobian matrix. From the perspective of zero-sequence networks, theoretically, even within the three-phase TR, some (e.g., Yg-D) belong to the ill condition, and some (e.g., Yg-Yg) belong to the well-condition. Therefore, checking the TR connection that hinders the convergence of the NR method by increasing the sensitivity of matrix calculation is necessary.

Therefore, this study calculated the condition number to check the sensitivity of the matrix calculation according to the TR types. Also, this study solved the singularities from the power flow calculation in the ill-condition, which includes the various cases defined above through the proposed MP-PI-based NR method, and details are in Section V.

V. CASE STUDIES

This study applied the MP-PI to the classical NR method to solve the singularities from the power flow calculation based on the NR method in the ill-condition systems. Therefore, this section confirmed the process of obtaining inverse matrices through the MP-PI and demonstrated the effectiveness of the MP-PI-based NR method calculation. Also, this section compares the power flow results using the proposed MP-PI-based approach with those from DIgSILENT Power Factory to verify the accuracy of the MP-PI-based NR algorithm. Since the classical NR-based power flow method often has poor convergence for unbalanced radial systems and systems with ungrounded TRs (e.g., D-connection), the IEEE 4-, 13-, 37-, and 69-bus systems with ill-conditions (e.g., radial systems with unbalanced loads and ungrounded TRs) were used as testbeds. And this study conducted two simulations for the 37-bus system. The IEEE 37-bus system was originally radial. However, this study created a 37-bus looped system with a slight modification on the IEEE 37-bus system to verify the performance of the MP-PI-based NR algorithm even in a looped system. That is, this study evaluated the proposed algorithm by adding three lines to the 37-bus system, simulating even for a looped system. In addition, this study defined this modified system as an IEEE 37-bus quasi-radial system. In addition, this study conducted simulations on the IEEE 69-bus system to verify the performance of the novel methodology proposed in this study on a large-scale radial system, which is a drawback of the NR method.

In addition, this study divided the case study into balanced and unbalanced simulations. Due to the different performances of classical NR methods for balanced and unbalanced power systems, this study separates the test systems into two. Also, since the power system usually operates within 30% of the imbalance rate, this study assumed the imbalance rate of the testbeds to be 30% (i.e., assumption of extreme cases) in the simulations for the unbalanced systems. And this study verified the performance of the MP-PI-based NR algorithm for systems with no load in the secondary side of TR, which is often considered ill-condition. All test feeders were radial or quasi-radial to prove the improvement in the disadvantages of the NR method. After each simulation, this study compared the results of the proposed MP-PI-based calculation algorithm and DIgSILENT Power Factory and calculated

TABLE 1. Case studies for validating the proposed moore-penrose pseudo-inverse-based newton-raphson method algorithm.

Case	Balancing condition	Test feeder
1	Balanced system	IEEE 4-bus system with delta load
2	Unbalanced system	
3	Balanced system	IEEE 4-bus system with wye load
4	Unbalanced system	
5	Balanced system	IEEE 13-node test feeder
6	Unbalanced system	
7	Balanced system	IEEE 37-bus radial system
8	Unbalanced system	
9	Balanced system	IEEE 37-bus quasi-radial system
10	Unbalanced system	
11	Balanced system	IEEE 69-bus system
12	Unbalanced system	

the maximum and average errors. TABLE 1 summarizes the systems tested in this study.

A. INVERSE MATRIX CALCULATION WITH MOOREPENROSE PSEUDO-INVERSE

This section provides the process to calculate the inverse matrix for a representative noninvertible (i.e., singular) matrix $\boldsymbol{Y}$ using the MP-PI matrix. MP-PI refers to a pseudo-inverse matrix that can play a role like an inverse matrix for a matrix in which an inverse matrix does not exist. Let

$$Y = \begin{bmatrix} -1 & 1 & 0 \\ 0 & -1 & 1 \\ 1 & 0 & -1 \end{bmatrix} \tag{20}$$

which has zero as the value of the determinant, the classical inversion is not available. Therefore, MP-PI should be used when such inversion is not possible. The MP-PI matrix can be obtained by following equation (17). The constituent SVD matrices are

$$U = \begin{bmatrix} 0.40824 & -0.70710 & 0.57735 \\ -0.81649 & 0.00000 & 0.57735 \\ 0.40824 & 0.70710 & 0.57735 \end{bmatrix}, \tag{21}$$

$$D = \begin{bmatrix} 1.73205 & 0.00000 & 0.00000 \\ 0.00000 & 1.73205 & 0.00000 \\ 0.00000 & 0.00000 & 1.73205 \end{bmatrix}, \tag{22}$$

and

$$V = \begin{bmatrix} 0.00000 & 0.81649 & -0.57735 \\ 0.70710 & -0.40824 & -0.57735 \\ -0.70710 & -0.40824 & -0.57735 \end{bmatrix}. \tag{23}$$

Hence the MP-PI-based inversion matrix is

$$Y^{+} = VD^{+}U^{T} = \begin{bmatrix} -0.33333 & 0.00000 & 0.33333 \\ 0.33333 & -0.33333 & 0.00000 \\ 0.00000 & 0.33333 & -0.33333 \end{bmatrix}. \tag{24}$$

The MP-PI can calculate the inversion of a non-invertible matrix that cannot be obtained by classical inversion.

TABLE 2. The admittance submatrix characteristics of three-phase transformers.

Primary	Secondary	Y_{PP}	Y_{SS}	Y_{PS}	Y_{SP}
$\boldsymbol{Y_g}$	$\boldsymbol{Y_g}$	Y_a	Y_a	$-Y_a$	$-Y_a$
$\boldsymbol{Y_g}$	$\boldsymbol{Y}$	Y_b	Y_b	$-Y_b$	$-Y_b$
$\boldsymbol{Y_g}$	$\boldsymbol{D}$	Y_a	Y_b	Y_c	Y^t_c
$\boldsymbol{Y}$	$\boldsymbol{Y_g}$	Y_b	Y_b	$-Y_b$	$-Y_b$
$\boldsymbol{Y}$	$\boldsymbol{Y}$	Y_b	Y_b	$-Y_b$	$-Y_b$
$\boldsymbol{Y}$	$\boldsymbol{D}$	Y_b	Y_b	Y_c	Y^t_c
$\boldsymbol{D}$	$\boldsymbol{Y_g}$	Y_b	Y_a	Y^t_c	Y_c
$\boldsymbol{D}$	$\boldsymbol{Y}$	Y_b	Y_b	Y^t_c	Y_c
$\boldsymbol{D}$	$\boldsymbol{D}$	Y_b	Y_b	$-Y_b$	$-Y_b$

TABLE 3. Admittance submatrix condition number with respect to transformer connection type.

Primary	Secondary	Transformer admittance matrix condition number
$\boldsymbol{Y_g}$	$\boldsymbol{Y_g}$	1.94e+18
$\boldsymbol{Y_g}$	$\boldsymbol{Y}$	1.05e+32
$\boldsymbol{Y_g}$	$\boldsymbol{D}$	3.10e+16
$\boldsymbol{Y}$	$\boldsymbol{Y_g}$	1.01e+32
$\boldsymbol{Y}$	$\boldsymbol{Y}$	1.01e+32
$\boldsymbol{Y}$	$\boldsymbol{D}$	7.20e+17
$\boldsymbol{D}$	$\boldsymbol{Y_g}$	1.95e+16
$\boldsymbol{D}$	$\boldsymbol{Y}$	9.73e+16
$\boldsymbol{D}$	$\boldsymbol{D}$	1.01e+32

B. TAP-CHANGING TRANSFORMER IMPEDANCE MATRIX CALCULATION USING MOORE-PENROSE PSEUDO-INVERSE

Tap-changing TRs can be used to maintain voltage magnitude 0.95 to 1.05 p.u. for unbalanced systems and reduce voltage imbalances [32]. This section presents a series of procedures to find the impedance matrix by inverting the non-invertible admittance matrix through the MP-PI. As an example of the calculation process, this study used a Yg-D tap changer TR. Yg-, Y-, and D-connections make nine types of 5-limb two-winding TRs. TABLE 2 shows submatrix characteristics for all nine TR combinations.

For example, Yg-D TR in TABLE 2 is composed of matrices such as

$$Y_{T,Yg-D} = \begin{bmatrix} Y_a & Y_c \\ Y_c^T & Y_b \end{bmatrix}. \tag{25}$$

And the matrices constituting the admittance submatrix in TABLE 2 are

$$Y_a = y_t \begin{bmatrix} 1 & 0 & 0 \\ 0 & 1 & 0 \\ 0 & 0 & 1 \end{bmatrix}, Y_b = \frac{y_t}{3} \begin{bmatrix} 2 & -1 & -1 \\ -1 & 2 & -1 \\ -1 & -1 & 2 \end{bmatrix},$$
$$Y_c = \frac{y_t}{\sqrt{3}} \begin{bmatrix} -1 & 1 & 0 \\ 0 & -1 & 1 \\ 1 & 0 & -1 \end{bmatrix}. \tag{26}$$

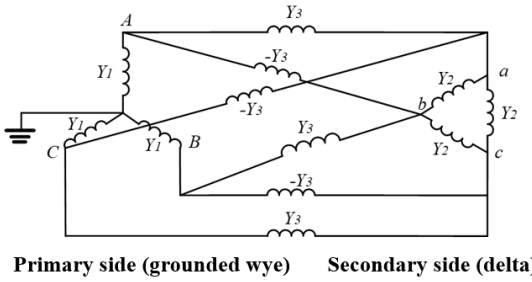

FIGURE 4. Admittance matrix of a tap-changing transformer, e.g., grounded wye-delta transformer.

TABLE 4. Jacobian matrix condition number with respect to transformer connection type and load.

Primary	Secondary	Load in bus 4	Load in bus 2
$\boldsymbol{Y_g}$	$\boldsymbol{Y_g}$	2.00e+154	5.23e+159
$\boldsymbol{Y_g}$	$\boldsymbol{Y}$	1.78e+160	1.32e+164
$\boldsymbol{Y_g}$	$\boldsymbol{D}$	1.16e+13	5.62e+160
$\boldsymbol{Y}$	$\boldsymbol{Y_g}$	5.85e+159	1.78e+157
$\boldsymbol{Y}$	$\boldsymbol{Y}$	2.04 e+160	4.34e+154
$\boldsymbol{Y}$	$\boldsymbol{D}$	1.16e+13	4.78e+149
$\boldsymbol{D}$	$\boldsymbol{Y_g}$	86.67	67.81
$\boldsymbol{D}$	$\boldsymbol{Y}$	2.26e+160	9.07e+14
$\boldsymbol{D}$	$\boldsymbol{D}$	1.15e+13	1.15e+15

Hence the admittance submatrix characteristics of the Yg-D TR can be expressed as

$$Y_T = y_t \begin{bmatrix} \frac{1}{\alpha^2} & 0 & 0 & \frac{-1}{\sqrt{3}\alpha\beta} & \frac{1}{\sqrt{3}\alpha\beta} & 0 \\ 0 & \frac{1}{\alpha^2} & 0 & 0 & \frac{-1}{\sqrt{3}\alpha\beta} & \frac{1}{\sqrt{3}\alpha\beta} \\ 0 & 0 & \frac{1}{\alpha^2} & \frac{1}{\sqrt{3}\alpha\beta} & 0 & \frac{-1}{\sqrt{3}\alpha\beta} \\ \frac{-1}{\sqrt{3}\alpha\beta} & 0 & \frac{1}{\sqrt{3}\alpha\beta} & \frac{2}{3\beta^2} & \frac{-1}{3\beta^2} & \frac{-1}{3\beta^2} \\ \frac{1}{\sqrt{3}\alpha\beta} & \frac{-1}{\sqrt{3}\alpha\beta} & 0 & \frac{-1}{3\beta^2} & \frac{2}{3\beta^2} & \frac{-1}{3\beta^2} \\ 0 & \frac{1}{\sqrt{3}\alpha\beta} & \frac{-1}{\sqrt{3}\alpha\beta} & \frac{-1}{3\beta^2} & \frac{-1}{3\beta^2} & \frac{2}{3\beta^2} \end{bmatrix} \quad (27)$$

where $\boldsymbol{y_t}$ represents a leakage admittance value in p.u.; the off-nominal tap ratios are expressed as α and β [33]; and Fig. 4 shows the corresponding three-phase magnetic coupling, with admittance components

$$Y_1 = \frac{y_t}{\alpha^2}, Y_2 = \frac{y_t}{3\beta^2}, Y_3 = \frac{y_t}{\sqrt{3}\alpha\beta}. \quad (28)$$

First, this study assumed specific values in off-nominal tap ratios for a clear understanding. If values of α and β (i.e., the off-nominal tap ratios) are two and three, respectively, the admittance submatrix based on TABLE 2 becomes in (29), as shown at the bottom of the next page.

And the inversion can be obtained for this non-invertible matrix to calculate MP-PI. The impedance matrix calculated through the MP-PI is as (21),

The exact inverse matrix cannot be calculated from the original inversion method because of the singularity. Thus, the original admittance submatrix $\boldsymbol{YT}$ cannot be returned by the double inversion processes, i.e., the double inverse of matrix $\boldsymbol{YT}$ (i.e., $(\boldsymbol{YT}^{-1})^{-1}$) calculation. However, the MP-PI returns the exact original matrix $\boldsymbol{YT}$ for the double inversion (i.e., $(\boldsymbol{YT}^{-1})^{-1}$). In other words, the MP-PI calculates the inversion more accurately than the classical inverse matrix process.

C. CHECKING THE CONDITION NUMBER

This section identifies condition numbers of the Jacobian matrix in an original NR algorithm, which performs iterative matrix calculations. Condition numbers of inversions indicate the sensitivity of the process of calculating the inversion. The inverse matrix calculation is sensitive when the condition number is high, implying increased relative error for the solution (i.e., ill-condition), whereas relative error for the solution decreases when the condition number is low (i.e., well-condition).

Therefore, this study confirmed the condition number of the admittance submatrix of nine types of TRs. TABLE 3 shows the condition numbers obtained for each admittance submatrix for all types of two-winding TRs that can be configured by combining the Yg-, Y-, and D-connections. The condition number increases when systems have a TR of combinations of the Yg- and Y-connection (e.g., Yg-Y, Y-Yg,), Y-connection on both sides (e.g., Y-Y), or D-connection on both sides (e.g., D-D).

This study confirmed the sensitivity of inverse calculation to check the condition number of the admittance submatrix. However, many singularities occur in the computation process of inversion of the Jacobian matrix. Thus, confirming the condition number of the Jacobian matrix of the power flow calculation according to the type of TR is necessary. The IEEE 4-bus system is a small-scale test feeder suitable for simulating various systems. In other words, the 4-bus system is appropriate to check the condition number of the Jacobian matrix according to all types of TRs. Thus, this study selected the IEEE 4-bus system as a testbed to confirm the condition number of the Jacobian matrix according to the type of TR. Fig. 5 is a 4-bus system, a simple radial system with one TR between buses 2 and 3, for checking the condition number of the Jacobian matrix.

In Fig. 5, loads are in buses 2 and 4, but it does not mean a system with two loads. In this study, simulations were carried out by assuming a load in bus 2 or bus 4 to check the sensitivity of the power system according to the presence of a load. In other words, since there were often cases of singularities when there was no load at the end of the unground side, this study checked the condition number of the Jacobian matrix for the ill-condition system by adjusting the location of the load in the 4-bus system. Thus, this study confirmed the condition number for the case where a load is on the primary and secondary sides of the TR, respectively.

TABLE 5 provides Jacobian matrix condition numbers for all TR combinations in the IEEE 4-bus system shown in Fig. 5. When a load is only in bus 4, presented in column 3 of TABLE 5, power flow only converged when the TR was a D-Yg connection or the secondary side of the TR was a

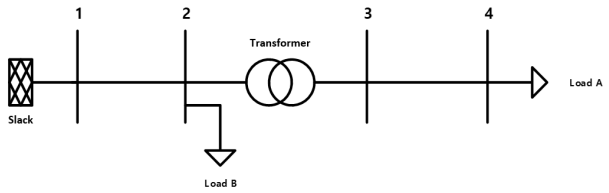

FIGURE 5. Single-line diagram of the IEEE 4-bus system for checking the condition number.

TABLE 5. Transformer data in the IEEE 4-bus system.

	MVA	kV (L-L) high	kV (L-L) low	R (p.u.)	X (p.u.)
TR	6	12.47	4.16	0.01	0.06

D-connection, i.e., Yg-D, Y-D, or D-D. When a load was only in bus 2, presented in column 4 of TABLE 5, power flow only converged when the TR primary side was a D-connection, i.e., D-Yg, D-Y, or D-D.

In addition, in the case of systems with Yg-D and Y-D TR, when comparing columns 3 and 4 in TABLE 4, if there is no load on the secondary side of the TR (i.e., load in bus 2), the condition number increases very significantly. In other words, this study confirmed that when D-connection is only on the secondary side of the TR (e.g., the Yg-D or Y-D), the singularity may be serious for a system with no load on the D-connection side.

The high condition number of the Jacobian matrix results in high sensitivity to inverse matrix calculations. For instance, TABLE 4 shows that in a system with a Yg-D TR, the power flow calculation converges when the load is on bus 4 (column 3), as the condition number of the Jacobian matrix is 1.16e+13. However, when the load is only on bus 2 (column 4), the condition number of the Jacobian matrix is 5.62e+160, and the power flow calculation does not converge. The Y-D TR also exhibits the same behavior as the Yg-D TR, where the presence of a load (i.e., no load D-side) may lead to an ill-conditioned system. Singularities frequently occur, and classical inversion is impossible in such systems due to high condition numbers. In such cases, the MP-PI calculation is required for inversion.

This study has confirmed the necessity of the MP-PI calculation by examining the condition numbers of the admittance submatrix and the Jacobian matrix. Even in small-scale radial or ground systems, existing inversion may not be suitable for power flow calculations. The sensitivity is generally high in systems with high condition numbers, as shown in TABLE 3 and TABLE 4. Thus, the MP-PI-based NR method is useful for power flow analysis in sensitive systems with high condition numbers. Even in simple systems, classical NR methods may result in singularity and power flow convergence failure. In such cases, the MP-PI-based NR method can be utilized for power flow analysis.

So far, this study separated case studies; calculated the MP-PI for a representative singular matrix; calculated the impedance matrices through the admittance matrix of tap-changing TR through the MP-PI; and confirmed condition numbers of the TR admittance submatrix and Jacobian matrices according to the type of TR. In addition, in the process, the necessity of the MP-PI-based NR method was confirmed, which supplemented the shortcomings of the NR method. In the next section, this study calculated power flows from test feeders to verify the convergence and accuracy of the MP-PI-based NR method.

D. IEEE 4-BUS SYSTEM

In this section, this study verified the power flow calculation result through the MP-PI-based NR algorithm. The first feeder for power flow calculation is the IEEE 4-bus system used to check the condition number in the previous section. This study confirmed the convergence of the proposed MP-PI-based algorithm for the IEEE 4-bus system, a small-scale and simple network. Fig. 6 is a single-line diagram of the IEEE 4-bus system. In TABLE 4, when a system with a Yg-D TR between buses 2 and 3 in the 4-bus system and the secondary side of the TR has no load (i.e., column 4

$$Y_T = \begin{bmatrix} 0.2500 & 0.0000 & 0.0000 & -0.0962 & 0.0962 & 0.0000 \\ 0.0000 & 0.2500 & 0.0000 & 0.0000 & -0.0962 & 0.0962 \\ 0.0000 & 0.0000 & 0.2500 & 0.0962 & 0.0000 & -0.0962 \\ -0.0962 & 0.0000 & 0.0962 & 0.0741 & -0.0370 & -0.0370 \\ 0.0962 & -0.0962 & 0.0000 & -0.0370 & 0.0741 & -0.0370 \\ 0.0000 & 0.0962 & -0.0962 & -0.0370 & -0.0370 & 0.0741 \end{bmatrix}. \tag{29}$$

$$Z_T = \begin{bmatrix} 2.6114 & 0.6943 & 0.6943 & -0.7379 & 0.7379 & 0.0000 \\ 0.6943 & 2.6114 & 0.6943 & 0.0000 & -0.7379 & 0.7379 \\ 0.6943 & 0.6943 & 2.6114 & 0.7379 & 0.0000 & -0.7379 \\ -0.7379 & 0.0000 & 0.7379 & 0.5680 & -0.2840 & -0.2840 \\ 0.7379 & -0.7379 & 0.0000 & -0.2840 & 0.5680 & -0.2840 \\ 0.0000 & 0.7379 & -0.7379 & -0.2840 & -0.2840 & 0.5680 \end{bmatrix}. \tag{30}$$

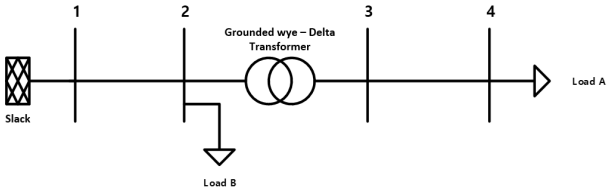

FIGURE 6. Single-line diagram of the IEEE 4-bus system.

in TABLE 4), the condition number increased significantly compared to the case where there was a load on the secondary side of the TR (i.e., column 3 in TABLE 4), and the power flow calculation with the classical NR method does not converge. Therefore, in this paragraph, this study selected the type of TR as Yg-D in the 4-bus system and confirmed the convergence of the MP-PI-based power flow calculation according to the presence of a load in the secondary side of TR (i.e., bus 4). TABLE 5 provides corresponding TR data. And this study assumed that the imbalance rate of the unbalanced system was 30%.

In TABLE 4, the condition number of the Jacobian matrix was high when there was no load on the secondary side (i.e., D-side) in Yg-D or Y-D TRs. Thus, the classical NR method-based power flow calculation does not converge. This study confirmed the condition number of the Jacobian matrix through the classical NR method and the proposed MP-PI-based NR method for a system with no load on the D-connection side, the secondary side of TR, in a 4-bus system with Yg-D TR. Fig. 7 shows the condition number of the Jacobian matrix based on the classical NR method. In Fig. 7, the above graph shows the condition number of the Jacobian matrix according to each iteration when the iteration progresses by about half. And the graph below in Fig. 7 shows the simulation results up to the maximum iteration. In other words, this study confirmed through Fig. 7 that as the number of iterations increases, the condition number of the Jacobian matrix increases to infinity. And the power flow calculation with the classical NR method did not converge. This means that in a case like Fig. 7, the classical NR method cannot be used to solve the power flow calculation.

Fig. 8 shows the simulation results when calculating power flow in the 4-bus system using the proposed MP-PI-based NR method. In Fig. 8, in the MP-PI-based calculation, the condition number of the Jacobian matrix decreased, and the power flow calculation converged as the iteration increased. Unlike the classical NR-based power flow calculation, the number of iterations was low with the MP-PI-based calculation, and the power flow calculation converged. For cases where the power flow calculation was not converged with the classical NR method, the power flow calculation with the proposed MP-PI-based NR method converged. The MP-PI-based method improved power flow convergence for the ill condition. Therefore, the MP-PI-based calculation proposed in this study is appropriate to improve the disadvantages of the classical NR method.

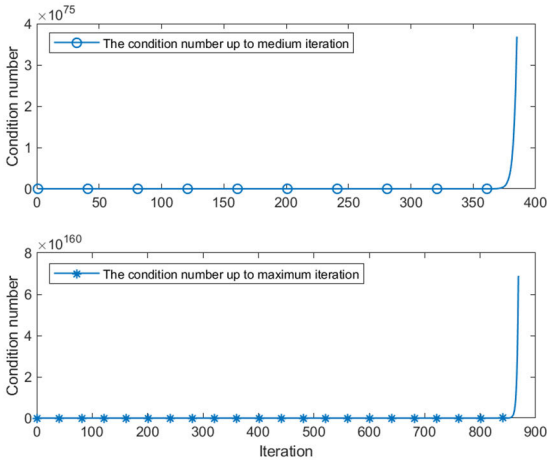

FIGURE 7. Condition number of the jacobian matrix based on the classical newton-raphson method.

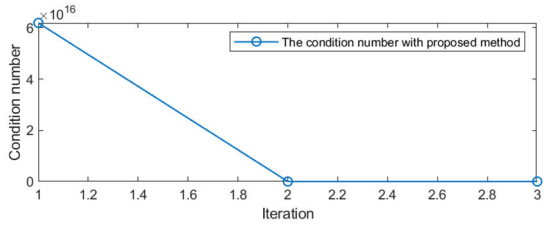

FIGURE 8. Condition number of the jacobian matrix based on the proposed newton-raphson method with moore-penrose Pseudo-inverse.

TABLE 6. Scenarios for the simulation of the IEEE 4-bus system.

Scenario	Balancing condition	Location of a load
1	Balanced system	Bus 4
2	Unbalanced system	
3	Balanced system	Bus 2
4	Unbalanced system	

Next, this study verified the accuracy of the proposed methodology by comparing the results of the MP-PI-based calculation with those of DIgSILENT. Like checking the condition number of the Jacobian matrix, Loads A and B are illustrated together in Fig. 6, but it means different systems (i.e., 4-bus systems with only Load A or Load B). And this study considered four cases for the 4-bus system: Load A was balanced or unbalanced, and Load B was balanced or unbalanced. Thus, the four simulations mean power flow calculation in the system with D-balanced load, D-unbalanced load, Y-balanced load, and Y-unbalanced load, respectively. TABLE 6 summarized the scenarios for simulation in the IEEE 4-bus system.

Fig. 9 and TABLE 7 compared the proposed MP-PI-based NR algorithm with DIgSILENT power flow results. The error defined in this study is the value by calculating the difference in voltage magnitude (p.u.) in the power flow calculation result through the proposed MP-PI-based NR method and DIgSILENT. And the error is the absolute value. First, in scenarios 1 and 3 for the balanced system, the error occurred

TABLE 7. Simulation results in the IEEE 4-bus system.

Location of a load	Error (p.u.)	Balanced system	Unbalanced system
Bus 4	Maximum	0.000006	0.000033
	Average	0.000003	0.000019
Bus 2	Maximum	0.000001	0.000028
	Average	0.000001	0.000015

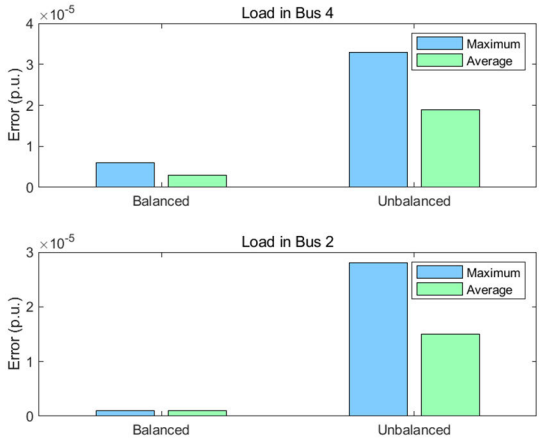

FIGURE 9. Simulation results in the IEEE 4-bus system.

at the sixth digit after the decimal point. On the other hand, in scenarios 2 and 4 for the unbalanced system, the error occurred at the fifth place after the decimal point. The error in scenarios 2 and 4 (i.e., the unbalanced system) increased compared to scenarios 1 and 3 (i.e., the balanced system). But in all four cases, the error was a low value of less than 0.004%. All four simulations in TABLE 6 converged, even when there was no load on the secondary side (i.e., the D-connection side of the TR). When tested on a simple 4-bus system, the convergence and accuracy of the MP-PI-based calculation were good.

E. IEEE 13-NODE TEST FEEDER

The IEEE 4-bus system used in the previous paragraph in this study is a basic system in which power flows in one direction from the slack to the load. However, unlike the 4-bus system, the 13-bus system in Fig. 10 has several buses that branch into four buses and is heavily loaded. These characteristics can often lead the power system to ill condition, making the calculation sensitive.

The IEEE 13-node test feeder is a small-scale system that operates at 4.16 kV and has relatively heavy loads in a short length. In other words, the 13-node test feeder is suitable for verifying the performance of the MP-PI-based algorithm in systems with heavy loads, radial structures, and unbalanced characteristics (i.e., ill conditions). This study selected the IEEE 13-node test feeder as the second testbed to confirm the performance of the MP-PI-based calculation in the system with various ill conditions than the 4-bus system. In addition, as in the case study of the IEEE 4-bus system, this study

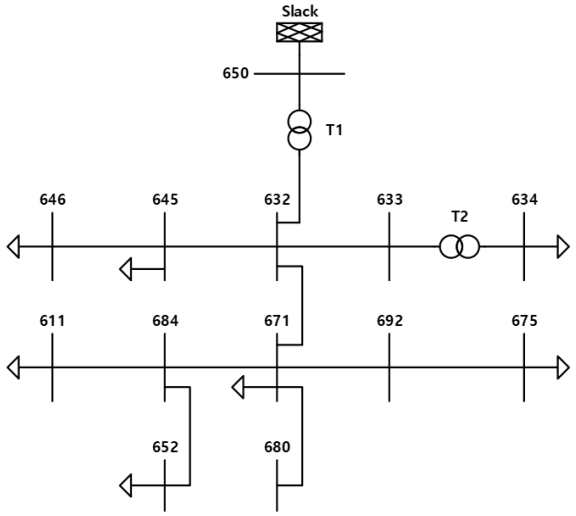

FIGURE 10. Single-line diagram of the IEEE 13-node test feeder.

TABLE 8. Transformer data in the IEEE 13-node test feeder.

	MVA	kV (L-L) high	kV (L-L) low	R (p.u.)	X (p.u.)
T1	5	115	4.16	0.08	0.1
T2	0.5	4.16	0.48	0.02	0.011

TABLE 9. Simulation results in the IEEE 13-node test feeder.

Error (p.u.)	Balanced system	Unbalanced system
Maximum	0.000085	0.000208
Average	0.000039	0.000072

divided simulations into cases for balanced and unbalanced systems.

This study modified the IEEE 13-node test feeder by eliminating the distributed load and capacitor bank from the original 13-node systems. Fig. 10 shows a modified 13-bus system with 13 buses, two TRs, and seven loads, where T1 and T2 are Yg-D and D-D TRs, respectively. TABLE 8 provides corresponding TR data. And this study assumed that the imbalance rate of the unbalanced system was 30%.

Fig. 11 and TABLE 9 shows the maximum and average error values of each when comparing power flow results of the MP-PI-based NR method and DIgSILENT in balanced and unbalanced systems. In the 13-node system, the maximum error occurred at the fifth place after the decimal point in the balanced system and at the fourth place after the decimal point in the unbalanced system, respectively. The average error was fifth place after the decimal point in both balanced and unbalanced systems. Compared to the simple 4-bus system, the error in the 13-bus system is increased. First, the 13-bus system had more ill conditions (e.g., more complex radial structure or heavy load) than the 4-bus system. A slightly more complex radial structure, a heavy load condition, and an unbalanced condition increase the error slightly. However, the maximum error in the unbalanced

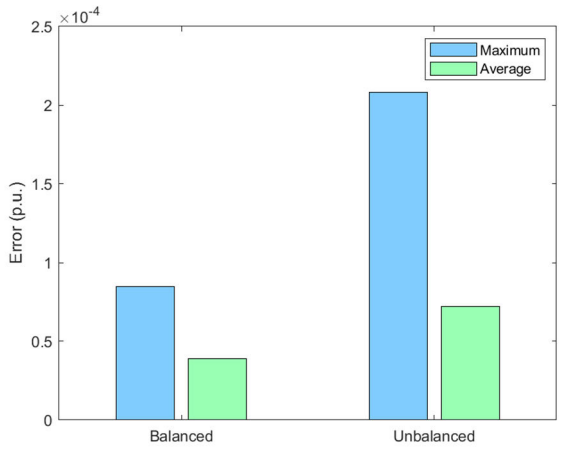

FIGURE 11. Simulation results in the IEEE 13-node test feeder.

13-bus system is 0.0208%, which is lower than 0.03%. That is, the accuracy of the MP-PI-based NR method proposed in this study was quite high.

In other words, when referring to the simulation results in the 13-bus system, the imbalance condition can lead the system to an ill condition. In addition, since the maximum and average errors slightly increased when compared with the simulation results of the 4-bus system, a more complex radial structure or a heavy load condition can increase the sensitivity of the power system.

F. IEEE 37-BUS RADIAL SYSTEM

The 4- and 13-bus systems are relatively small-scale systems suitable for testing various systems, but the 4- and 13-bus systems are not appropriate because the systems have simple structures to be applied in actual systems. The IEEE 37-bus test feeder is a real-world grid in California that operates at 4.8 kV. Therefore, IEEE 37-bus feeder is suitable for testing the MP-PI-based NR methods in an actual power system network.

Fig. 12 is a single-line diagram of the 37-bus test feeder. This feeder has two D-D TRs, and the entire system is ungrounded. Also, the secondary side of the D-D TR, denoted as XFM, between buses 709 and 775 has no load. The IEEE 37-bus feeder is a system that has the characteristics of representative ill-condition systems like radial distribution systems, unbalanced systems, no load condition on the secondary side of the D-side of TRs, and ungrounded grids. Therefore, this study verified the performance and accuracy of the proposed MP-PI-based NR method in the IEEE 37-bus system, including various ill conditions. As in the previous case studies, this study verified the accuracy of the MP-PI-based NR method for each of the two cases about balanced and unbalanced systems. Therefore, this study was conducted by dividing the simulation of the 37-bus radial system into balanced and unbalanced systems. And this study assumed that the imbalance rate of the unbalanced system was 30%. TABLE 10 provides corresponding TR data.

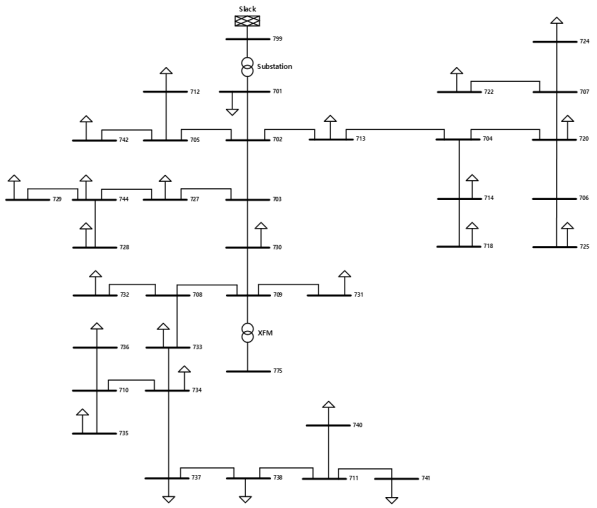

FIGURE 12. Single-line diagram of the IEEE 37-bus radial test feede.

TABLE 10. Transformer data in the IEEE 37-bus radial test feeder.

	MVA	kV (L-L) high	kV (L-L) low	R (p.u.)	X (p.u.)
Substation	2.5	230	4.8	0.02	0.08
XFM	0.5	4.8	0.48	0.0009	0.00181

TABLE 11. Simulation results in the IEEE 37-bus radial test feeder.

Error (p.u.)	Balanced system	Unbalanced system
Maximum	0.000019	0.000012
Average	0.000017	0.000007

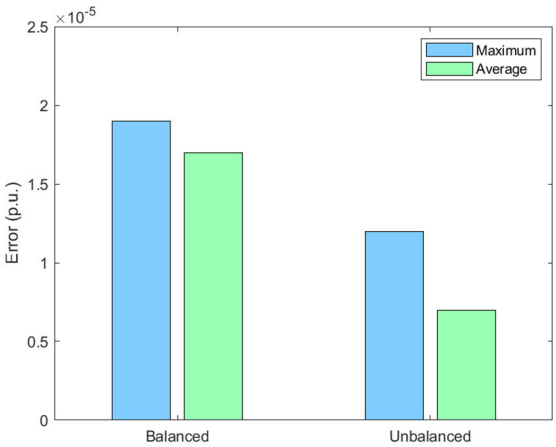

FIGURE 13. Simulation results in the IEEE 37-bus quasi-radial system.

Fig. 13 and TABLE 11 shows the maximum and average error values of each when comparing the power flow results of the MP-PI-based NR method and DIgSILENT in the balanced and unbalanced systems. First, in the balanced simulation, the maximum and average error values of the 37-bus system were 0.000019 and 0.000017 p.u., respectively, and in the unbalanced system with a 30% of

imbalance rate, the maximum and average error values were 0.000012 and 0.000007, respectively. The maximum and average errors for the balanced and unbalanced systems occurred at five or sixth decimal places and were both low values.

The simulation results in the 13-bus system show higher errors in the unbalanced system than in the balanced system. In other words, the imbalance condition often leads the system to ill-condition and makes the calculation sensitive. However, simulation results for the 37-bus radial system were different. Rather, the error was slightly lower in the unbalanced system. In other words, the MP-PI-based calculation effectively solved the singularity caused by imbalance. And this case study shows that the reason for the higher error in the IEEE 13-node test feeder at the unbalanced condition is not caused by an unbalanced condition.

And in the MP-PI-based calculation, the maximum error in both the balanced and unbalanced systems did not exceed 0.002%. In other words, the power flow calculation based on the MP-PI-based NR method was accurate even in the radial system closest to the actual power system. This study revealed that the MP-PI-based NR method improved the limitations of the NR method calculation through simulation on the 37-bus radial system.

G. IEEE 37-BUS QUASI-RADIAL SYSTEM

The MP-PI-based NR method proposed in this study was intended to improve the limitations of the NR method (i.e., the singularity) and focused on verification in the radial system (i.e., the shortcoming of the power flow calculation with the NR method). However, actual power systems may have heavily looped structures as well as radial structures. Thus, simulation and verification of quasi-radial systems with loops are also required. Therefore, this study created an IEEE 37-bus quasi-radial system by slightly modifying the IEEE 37-bus radial system. Three lines are added to the original IEEE 37-bus feeder. The data for the additional lines are in TABLE 12. This study assumed that the impedance of all three newly added lines was the same.

Fig. 14 shows a modified 37-bus quasi-radial system. The added links are indicated by the dotted lines. The additional three lines in TABLE 12 to the IEEE 37-bus radial system in Fig. 12 resulted in a quasi-radial system with three loops. In other words, the IEEE 37-bus quasi-radial system has three additional loops while maintaining all the structures of the original 37-bus system. The IEEE 37-bus quasi-radial system is an appropriate feeder for verifying the convergence and accuracy of the MP-PI-based NR calculation in near-actual quasi-radial structures.

Fig. 15 and TABLE 13 shows the difference (i.e., error in terms of voltage magnitude) from DIgSILENT when calculating the power flow through the proposed MP-PI-based NR method for the IEEE 37-bus quasi-radial system. Although the maximum and average errors are slightly reduced compared to the IEEE 37-bus radial system, it is not much different. In addition, the error in the unbalanced system in the

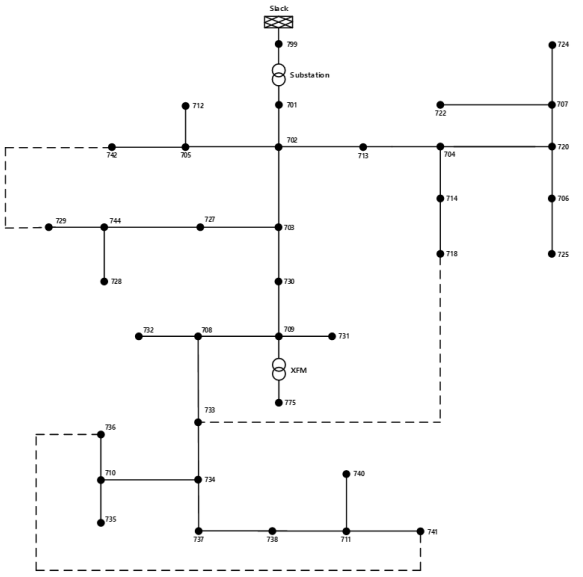

FIGURE 14. Single-line diagram of the IEEE 37-bus quasi-radial system.

TABLE 12. Additional line data in the IEEE 37-bus quasi-radial test feeder.

Location of the additional line	0-sequence impedance	1, 2-sequence impedance
Between buses 718 and 733	0.01 + j 0.001 [ohm/km]	0.01 + j 0.001 [ohm/km]
Between buses 729 and 742		
Between buses 736 and 741		

TABLE 13. Simulation results in the IEEE 37-bus quasi-radial test feeder.

Error (p.u.)	Balanced system	Unbalanced system
Maximum	0.000018	0.000008
Average	0.000016	0.000007

IEEE quasi-radial 37-bus system was slightly lower than that in the balanced system, as shown in the simulation results in the IEEE 37-bus radial system. In addition, compared to DIgSILENT, the error was low, and the accuracy of the MP-PI-based calculation was high. In other words, the MP-PI-based NR method proposed in this study completed not only radial but also power flow analysis in the quasi-radial system.

H. IEEE 69-BUS SYSTEM

Finally, this study aimed to evaluate the effectiveness of the proposed MP-PI-based methodology for the IEEE 69-bus system, a large-scale radial system commonly used in power system analysis. In addition, this study used a slightly modified version to verify the performance of the proposed methodology for singularity problems caused by TR connections and imbalance. Fig. 16 shows a modified 69-bus system used as a test feeder in this study. TABLE 14 shows the data for the three TRs. Three Yg-D TR were added at the location where bus 3 branches to buses 4, 28, and 36, respectively. With these modifications, this study was able to evaluate the effectiveness of the proposed methodology for a system

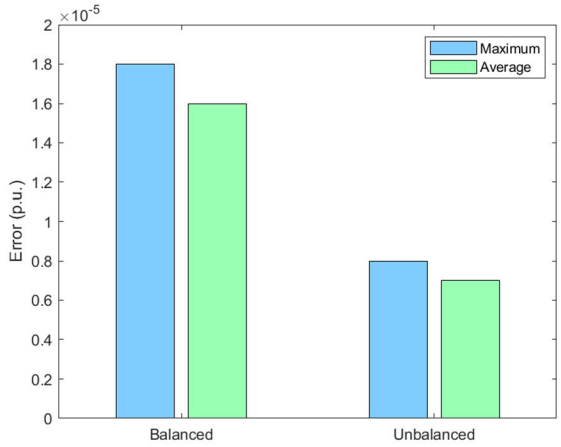

FIGURE 15. Simulation results in the IEEE 37-bus quasi-radial system.

TABLE 14. Transformer data in the IEEE 69-bus system.

	MVA	kV (L-L) high	kV (L-L) low	R (p.u.)	X (p.u.)
TR 3-4	10	13.8	13.8	0.0007	0.0018
TR 3-28	10	13.8	13.8	0.0023	0.0056
TR 3-36	10	13.8	13.8	0.0023	0.0056

TABLE 15. Simulation results in the IEEE 69-bus system.

Error in p.u.	Balanced system	Unbalanced system
Maximum	0.000035	0.000053
Average	0.000008	0.000031

containing three TRs, 48 loads, and 69 buses. The modified 69-bus system was used to validate this study's improvements to the limitations of the classical NR method in large-scale radial distribution systems.

The simulation results presented in Fig. 17 and TABLE 15 show the comparison of the performance of the proposed methodology for the IEEE 69-bus system. For the balanced systems, the maximum and average errors were found to be 0.000035 and 0.000008, respectively. For unbalanced systems, the maximum and average errors were slightly larger, at 0.000053 and 0.000031, respectively. In both the balanced and unbalanced systems, the error occurred in the fifth or sixth decimal place. This result indicates that the proposed methodology performs very well for balanced and unbalanced systems, with very small errors. Overall, these results indicate that the proposed methodology is effective for calculating power flow in the IEEE 69-bus system, with very small errors for balanced systems and only slightly larger errors for unbalanced systems. This suggests that the methodology is a useful tool for power flow calculation, particularly for large-scale radial systems like the IEEE 69-bus system.

VI. DISCUSSION

This study verified the performance of the MP-PI-based NR for systems with various ill conditions. TABLE 16 summarizes the results of the case studies. All twelve simulations

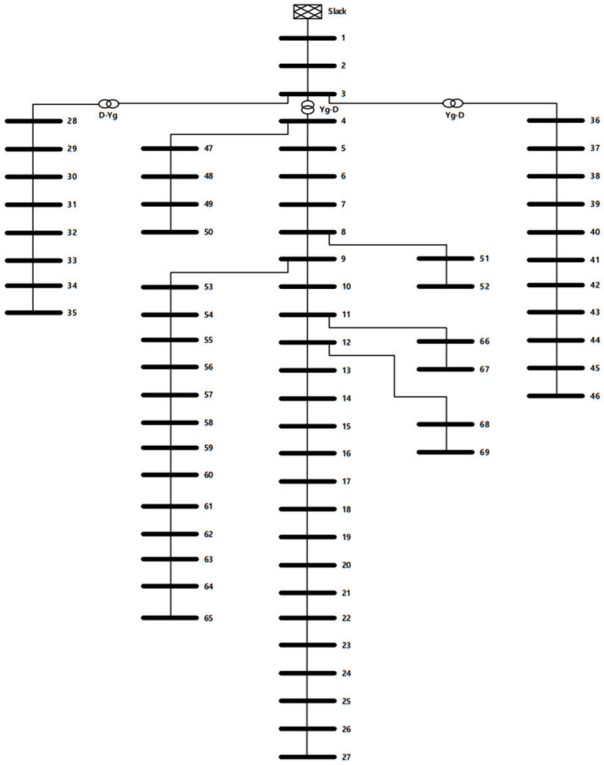

FIGURE 16. Single-line diagram of the modified IEEE 69-bus system.

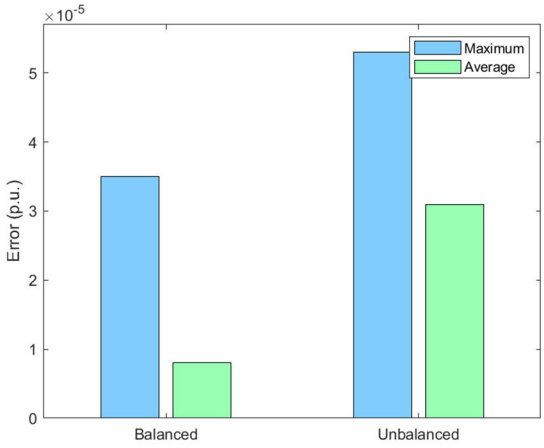

FIGURE 17. Simulation results in the IEEE 69-bus system.

converged using the proposed MP-PI-based NR algorithm, with high accuracy for balanced and unbalanced systems. In the 4-bus system, the maximum error was lower than 0.003% in both the balanced and unbalanced systems. In the 13-node system, maximum errors occurred at the fifth and fourth places below the decimal point in the balance and unbalance systems, respectively, and the unbalanced system had a higher error than the balanced system. In the 37-bus system, the maximum errors in both the balanced and unbalanced systems remained similar (0.000019, 0.000012 p.u.), and all these values were less than 0.002%. And in the

TABLE 16. Simulation results for the final discussion.

Testbed	Balancing condition	Error (p.u.)	
		Maximum	Average
4-bus system with Y-load	Balanced system	0.000001	0.000001
	Unbalanced system	0.000028	0.000015
4-bus system with D-load	Balanced system	0.000006	0.000003
	Unbalanced system	0.000033	0.000019
13-node system	Balanced system	0.000085	0.000039
	Unbalanced system	0.000208	0.000072
37-bus radial system	Balanced system	0.000019	0.000017
	Unbalanced system	0.000012	0.000007
37-bus quasi-radial system	Balanced system	0.000018	0.000016
	Unbalanced system	0.000008	0.000007
69-bus system	Balanced system	0.000035	0.000008
	Unbalanced system	0.000053	0.000031

IEEE 37-bus quasi-radial system, the maximum errors were 0.000018 and 0.000008 p.u., respectively, in the balanced and unbalanced systems. Even in the IEEE 69-bus system (i.e., a large-scale radial system), the maximum error was as low as 0.000035 and 0.000053 p.u. for balanced and unbalanced systems, respectively.

As a result, in small-scale systems (i.e., 4- or 13-bus systems), imbalance may lead the system to ill conditions, preventing the convergence of power flow calculation. However, in the 37-bus radial or quasi-radial systems, the balanced simulation resulted in a higher error than the unbalanced simulation. Even in the IEEE 69-bus system, the maximum error was nearly identical for balanced and unbalanced systems. In other words, in the large-scale system, the effect of the imbalance was not significant. The testbed with the highest error is the IEEE 13-node test feeder. This system (i.e., the IEEE 13-node test feeder) is a small-scale system and is a heavy-load system. In other words, heavy load conditions can also make the system sensitive in small-scale systems. Therefore, as future research, it is necessary to apply the proposed MP-PI-based calculation method too heavily loaded systems in various small-scale grids, reduce the error rate to the fifth decimal place, and conduct research to further improve the accuracy and understand the principle.

MP-PI-based calculation showed good convergence characteristics in all 4-, 13-, 37-bus radial, 37-bus quasi-radial, and 69-bus systems. In addition, as a result of the power flow calculation of twelve simulations, the maximum error was low at 0.02%. In other words, this study completed convergence improvement and accuracy verification through MP-PI-based NR method calculation.

Fig. 18 shows the maximum and average errors of the MP-PI-based calculations for all 12 simulations performed in this study, which allows comparing the results of all the simulations. The highest errors were observed in the unbalanced 13-bus system, but the error values were low in all cases. This study successfully solved the disadvantages of the classical NR method and verified the accuracy of the proposed MP-PI-based NR method. Although the overall error rate is low, research is needed to analyze the factors that affect the accuracy of MP-PI-based NR methods.

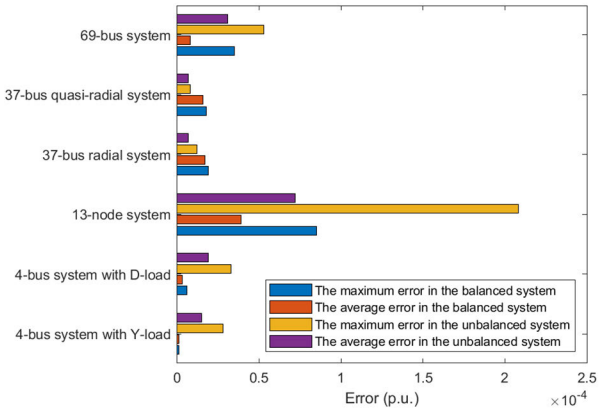

FIGURE 18. The maximum and average errors for all twelve simulations.

TABLE 17. Simulation time of the classical newton-raphson and the proposed newton-raphson methods.

Testbed	Balancing condition	Simulation time (s)	
		Classical Newton - Raphson	Proposed Newton - Raphson
4-bus system with Y-load	Balanced system	0.247361	0.241622
	Unbalanced system	0.248257	0.241778
4-bus system with D-load	Balanced system	0.252260	0.257895
	Unbalanced system	0.251870	0.258430
13-node system	Balanced system	0.351645	0.349244
	Unbalanced system	0.346863	0.353512
37-bus radial system	Balanced system	-	0.404696
	Unbalanced system	0.392495	0.425716
37-bus quasi-radial system	Balanced system	-	0.430194
	Unbalanced system	-	0.421216
69-bus system	Balanced system	-	0.527498
	Unbalanced system	-	0.520293

TABLE 17 shows the simulation times for calculating power flow solutions using the classical NR and proposed MP-PI-based NR methods on different power systems. The simulation times were averaged over ten runs to obtain the reported values. The systems tested include the IEEE 4-,13-, 37-bus radial, 37-bus quasi-radial, and 69-bus systems.

As in TABLE 17, for the IEEE 4-bus and 13-node systems, both classical NR and proposed MP-PI-based methods yield similar simulation times. However, as the size of the system increases, the power flow calculation based on the classical NR method does not converge, and no solution is obtained. However, the MP-PI-based calculation proposed in this study converges to obtain a power flow calculation solution. Overall, the simulation time did not vary significantly between systems and methods, but the MP-PI-based computation proposed in this study is valuable in that it can compute solutions that could not be computed by the classical NR method.

VII. CONCLUSION

This study has identified various cases in which singularities can occur in the power flow calculation process using the classical NR method through condition numbers. To address

TABLE 18. Comparision of the classical newton-raphson and the proposed newton-raphson methods in the balanced systems.

Testbed	Error (%)		Simulation time (s)	
	Maximum	Average	Classical Newton-Raphson	Proposed Newton-Raphson
4-bus system with Y-load	0.00001	0.00001	0.247361	0.241622
4-bus system with D-load	0.00006	0.00003	0.252260	0.257895
13-node system	0.00033	0.00039	0.351645	0.349244
37-bus radial system	0.00019	0.00017	-	0.404696
37-bus quasi-radial system	0.00018	0.00016	-	0.430194
69-bus system	0.00035	0.00008	-	0.527498

TABLE 19. Comparision of the classical newton-raphson and the proposed newton-raphson methods in the unbalanced systems.

Testbed	Error (%)		Simulation time (s)	
	Maximum	Average	Classical Newton-Raphson	Proposed Newton-Raphson
4-bus system with Y-load	0.000028	0.000015	0.248257	0.241778
4-bus system with D-load	0.000033	0.000019	0.251870	0.258430
13-node system	0.000208	0.000072	0.346863	0.353512
37-bus radial system	0.000012	0.000007	0.392495	0.425716
37-bus quasi-radial system	0.000008	0.000007	-	0.421216
69-bus system	0.000053	0.000031	-	0.520293

the singularity problem, this study proposed a novel and robust MP-PI-based NR algorithm that applies to representative ill conditions. This study demonstrates an MP-PI-based calculation method that can calculate power flow more accurately by improving the performance of the NR method on unbalanced radial and heavy-load systems. Unlike other studies that focus on solving singularity problems, this study aims to improve the overall performance of the classical NR method. The proposed MP-PI-based NR algorithm significantly improved convergence and reduced the error rate to less than 0.02%. This study proposes an algorithm that can simultaneously handle various adverse conditions that have not been sufficiently addressed in existing research. Additionally, this study validated the performance of the proposed algorithm using the DIgSILENT software and showed that it outperforms the classical NR method on unbalanced radial and heavy-load systems. When comparing the results of the power flow calculation of the methodology proposed in this study with DIgSILENT, the overall error rate is low, but the error rate for the case study of the IEEE 13-node test feeder is about 0.02%, which is relatively high compared to other case study results. An in-depth analysis of the reasons for this relatively high error rate is needed. In other words, further research is needed to analyze the factors that affect the accuracy of the MP-PI-based NR method.

APPENDIX

This study conducted various case studies using the proposed MP-PI-based NR method. IEEE 4-, 13-, 37-, and 69-bus systems were modeled, and the power flow calculation results were compared with DIgSILENT (i.e., the robust power flow analysis software). The metric for comparing the power flow calculation results is the voltage magnitude. TABLE 18 and TABLE 19 shows the simulation times of the classical NR and the proposed NR method in balanced and unbalanced systems and the maximum and average errors of the proposed MP-PI-based method.

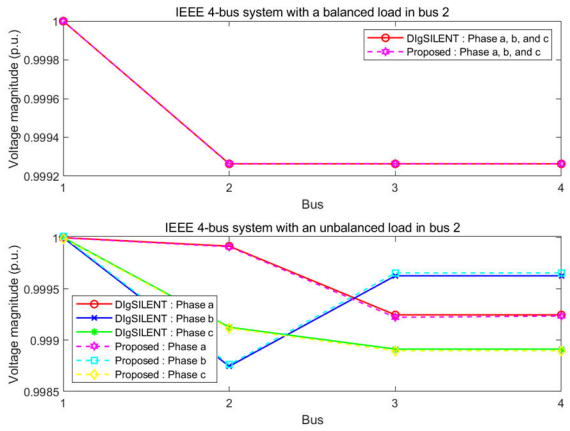

FIGURE 19. Simulation results in the IEEE 4-bus system with a wye-load.

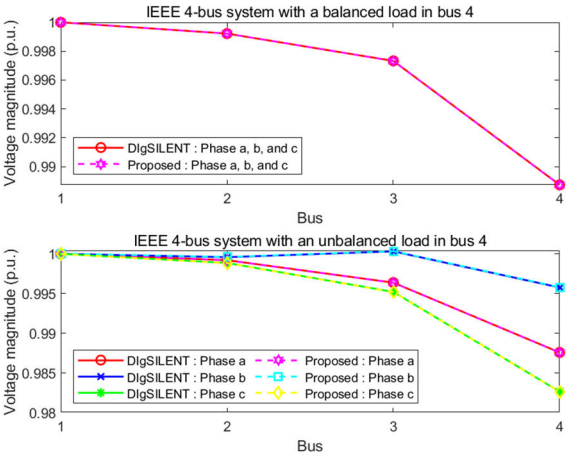

FIGURE 20. Simulation results in the IEEE 4-bus system with a delta-load.

And this study visualized the power flow calculation results based on the MP-PI-based NR method. Fig. 19, Fig. 20, Fig. 21, Fig. 22, Fig. 23, and Fig. 24 show the power flow calculation results for the case studies in this study. The x-axis represents each bus number, and the y-axis

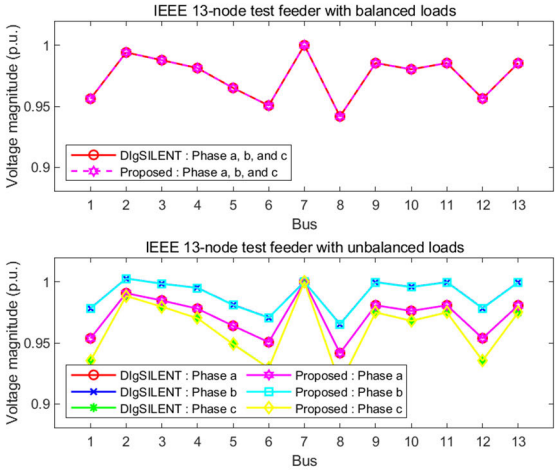

FIGURE 21. Simulation results in the IEEE 13-node test feeder.

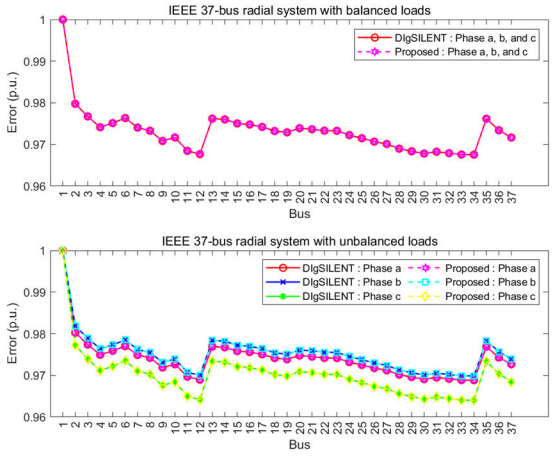

FIGURE 22. Simulation results in the IEEE 37-bus radial system.

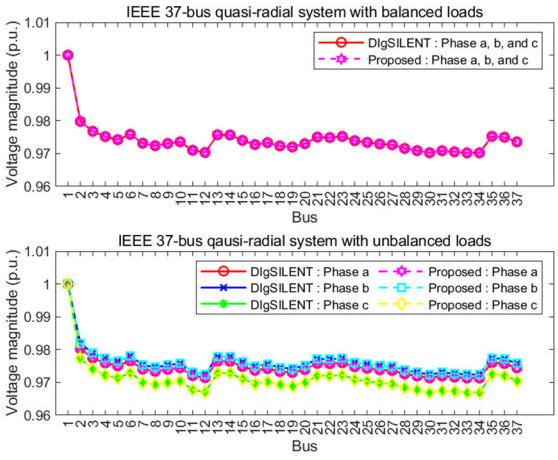

FIGURE 23. Simulation results in the IEEE 37-bus quasi-radial system.

represents the error of the voltage magnitude on that bus. The bus numbers are different from the bus numbers in the single-line diagram shown in the case study section and are

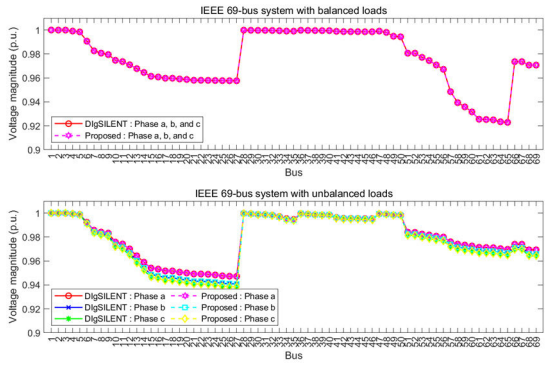

FIGURE 24. Simulation results in the IEEE 69-bus system.

given sequentially and in batches starting from 1 to represent the error of all buses. For the balanced system, the magnitudes of the voltages on A, B, and C are the same, so the voltage magnitude of the phases a, b, and c are shown in one graph. For the unbalanced system, the voltage magnitudes of phases a, b, and c are different, so they are shown separately. Also, the simulation results of DIgSILENT and the proposed method are shown as solid and dotted lines, respectively. The accuracy of the power flow calculation results is high for all 12 case studies in this study.

REFERENCES

[1] W. F. Tinney and C. E. Hart, "Power flow solution by Newton's method," *IEEE Trans. Power App. Syst.*, vol. PAS-86, no. 11, pp. 1449–1460, Nov. 1967.

[2] M. Abokrisha, A. Diaa, A. Selim, and S. Kamel, "Development of Newton-Raphson power-flow method based on second order multiplier," in *Proc. 19th Int. Middle East Power Syst. Conf. (MEPCON)*, Dec. 2017, pp. 976–980.

[3] V. Veerasamy, N. I. A. Wahab, R. Ramachandran, S. Kamel, M. L. Othman, H. Hizam, and R. Farade, "Power flow solution using a novel generalized linear Hopfield network based on Moore–Penrose pseudoinverse," *Neural Comput. Appl.*, vol. 33, no. 18, pp. 11673–11689, Sep. 2021.

[4] S. Iwamoto and Y. Tamura, "A load flow calculation method for ill-conditioned power systems," *IEEE Trans. Power App. Syst.*, vol. PAS-100, no. 4, pp. 1736–1743, Apr. 1981.

[5] Z. Liu, X. Zhang, M. Su, Y. Sun, H. Han, and P. Wang, "Convergence analysis of Newton-Raphson method in feasible power-flow for DC network," *IEEE Trans. Power Syst.*, vol. 35, no. 5, pp. 4100–4103, Sep. 2020.

[6] F. Milano, "Continuous Newton's method for power flow analysis," *IEEE Trans. Power Syst.*, vol. 24, no. 1, pp. 50–57, Feb. 2009.

[7] K. A. Al-Anbarri, "Calculation of the bus voltages of a power system based on a swarm artificial intelligence technique," *AIP Conf.*, vol. 2386, no. 1, 2022, Art. no. 040005.

[8] R. Pourbagher and S. Y. Derakhshandeh, "Application of high-order Levenberg–Marquardt method for solving the power flow problem in the ill-conditioned systems," *IET Gener., Transmiss. Distrib.*, vol. 10, no. 12, pp. 3017–3022, Sep. 2016.

[9] D. Rajicic and A. Bose, "A modification to the fast decoupled power flow for networks with high R/X ratios," *IEEE Trans. Power Syst.*, vol. 3, no. 2, pp. 743–746, May 1988.

[10] B. Gasbaoui and B. Allaoua, "Ant colony optimization applied on combinatorial problem for optimal power flow solution," *Leonardo J. Sci.*, vol. 14, pp. 1–17, Jan. 2009.

[11] Y. Zhang, J. Lin, and C. Li, "A three-phase power flow algorithm for ungrounded network based on constraints of zero-sequence components," *Int. J. Electr. Power Energy Syst.*, vol. 145, Feb. 2023, Art. no. 108676.

[12] D. Thukaram, H. M. W. Banda, and J. Jerome, "A robust three phase power flow algorithm for radial distribution systems," *Electr. Power Syst. Res.*, vol. 50, pp. 227–236, Jun. 1999.

[13] D. A. Alves, L. C. P. D. Silva, C. A. Castro, and V. F. D. Costa, "Continuation fast decoupled power flow with secant predictor," *IEEE Trans. Power Syst.*, vol. 18, no. 3, pp. 1078–1085, Aug. 2003.
[14] R. Pourbagher, S. Y. Derakhshandeh, and M. E. H. Golshan, "An adaptive multi-step Levenberg-Marquardt continuation power flow method for voltage stability assessment in the ill-conditioned power systems," *Int. J. Electr. Power Energy Syst.*, vol. 134, Jan. 2022, Art. no. 107425.
[15] M. Tostado, S. Kamel, and F. Jurado, "Developed Newton-raphson based predictor-corrector load flow approach with high convergence rate," *Int. J. Electr. Power Energy Syst.*, vol. 105, pp. 785–792, Feb. 2019.
[16] K. K. Dewangan and A. K. Panchal, "Power flow analysis using successive approximation and adomian decomposition methods with a new power flow formulation," *Electr. Power Syst. Res.*, vol. 211, Oct. 2022, Art. no. 108190.
[17] F. D. Freitas and L. N. Oliveira, "Conditioning step on the initial estimate when solving ill-conditioned power flow problems," *Int. J. Electr. Power Energy Syst.*, vol. 146, Mar. 2023, Art. no. 108772.
[18] R. Mukhopadhyay and M. R. Talipov, "Efficient Newton-Raphson/singular value decomposition-based optimization scheme with dynamically updated critical condition number for rapid convergence of weighted histogram analysis method equations," *J. Comput. Chem.*, vol. 41, no. 3, pp. 240–246, Jan. 2020.
[19] G. A. N. Mbamalu, M. E. El-Hawary, and F. El-Hawary, "A pseudo-inverse-based probabilistic power flow approach," *Electr. Mach. Power Syst.*, vol. 23, no. 2, pp. 107–118, Mar. 1995.
[20] J. Bogovič and M. Pantoš, "Probabilistic three-phase power flow in a distribution system applying the pseudo-inverse and cumulant method," *J. Electr. Eng.*, vol. 73, no. 2, pp. 124–131, Apr. 2022.
[21] M. F. Allam and M. A. Laughton, "The use of pseudo and oblique pseudo-inverse matrices in power system state estimation algorithms," *Int. J. Control*, vol. 24, no. 5, pp. 661–671, Nov. 1976.
[22] T. R. Fernandes, T. R. Ricciardi, R. S. Silva, and M. C. Almeida, "Contributions to the sequence-decoupling compensation power flow method for distribution system analysis," *IET Gener., Transmiss. Distrib.*, vol. 13, no. 5, pp. 583–594, Mar. 2019.
[23] X.-P. Zhang and H. Chen, "Asymmetrical three-phase load-flow study based on symmetrical component theory," *IEE Proc.-Gener. Transmiss. Distrib.*, vol. 141, no. 3, pp. 248–252, May 1994.
[24] I. Džafić, R. A. Jabr, and H. T. Neisius, "Transformer modeling for three-phase distribution network analysis," *IEEE Trans. Power Syst.*, vol. 30, no. 5, pp. 2604–2611, Sep. 2015.
[25] M. Bazrafshan and N. Gatsis, "Comprehensive modeling of three-phase distribution systems via the bus admittance matrix," *IEEE Trans. Power Syst.*, vol. 33, no. 2, pp. 2015–2029, Mar. 2018.
[26] R. Pourbagher and S. Y. Derakhshandeh, "A powerful method for solving the power flow problem in the ill-conditioned systems," *Int. J. Electr. Power Energy Syst.*, vol. 94, pp. 88–96, Jan. 2018.
[27] T. Ochi, Y. Nonaka, D. Yamashita, K. Koyanagi, and R. Yokoyama, "Reliable power flow calculation with improved convergence characteristics for distribution systems," in *Proc. IEEE PES Innov. Smart Grid Technol.*, May 2012, pp. 1–6.
[28] S. Mallick, D. V. Rajan, S. S. Thakur, P. Acharjee, and S. P. Ghoshal, "Development of a new algorithm for power flow analysis," *Int. J. Electr. Power Energy Syst.*, vol. 33, no. 8, pp. 1479–1488, Oct. 2011.
[29] P. Courrieu, "Fast computation of Moore-penrose inverse matrices," 2008, *arXiv:0804.4809*.
[30] J. Zhao, J. Song, X. Li, and J. Kang, "A study on EEG feature extraction and classification in autistic children based on singular spectrum analysis method," *Brain Behav.*, vol. 10, no. 12, p. e01721, Dec. 2020.
[31] J. C. A. Barata and M. S. Hussein, "The Moore–Penrose pseudoinverse: A tutorial review of the theory," *Brazilian J. Phys.*, vol. 42, nos. 1–2, pp. 146–165, Apr. 2012.
[32] I. Kim, "A method of modeling tap-changing transformers for power-flow and short-circuit analysis studies," in *Proc. IEEE Region Conf. (TENCON)*, Oct. 2018, pp. 0772–0775.
[33] T.-H. Chen, M.-S. Chen, T. Inoue, P. Kotas, and E. A. Chebli, "Three-phase cogenerator and transformer models for distribution system analysis," *IEEE Trans. Power Del.*, vol. 6, no. 4, pp. 1671–1681, Oct. 1991.

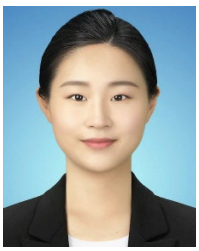

JIYEON JANG received the B.S. degree from the Department of Electrical Engineering, Inha University, Incheon, South Korea, in 2022, where she is currently pursuing the M.S. degree with the Department of Electrical and Computer Engineering. Her major research interests include the transient stability analysis of grids under penetration of distributed power sources and the performance improvement of power flow calculation algorithms.

DOHUN KIM received the B.S. degree from the Department of Electrical Engineering, Inha University, Incheon, South Korea, in 2020, and the M.S. degree from the Department of Electrical and Computer Engineering, Inha University. His major research interest includes the development of power flow calculation algorithms.

INSU KIM (Member, IEEE) received the Ph.D. degree from the Georgia Institute of Technology, Atlanta, in 2014. He is currently an Associate Professor in electrical engineering with Inha University, South Korea. His major research interests include analyzing the impact of stochastically distributed renewable energy resources, such as photovoltaic systems, wind farms, and microturbines on distribution networks, examining the steady-state and transient behavior of distribution networks under active and reactive power injection by distributed generation systems, and improving power-flow, short-circuit, and harmonic analysis algorithms.